Detection and Location of a Partial Blockage in a Pipeline Using Damping of Fluid Transients

Xiao-Jian Wang[1], Martin F Lambert[2], Angus R Simpson, M.ASCE[3]

Abstract:

The effects of a partial blockage on pipeline transients are investigated analytically. A partial blockage is simulated using an orifice equation and the influence of the blockage on the unsteady pipe flow is considered in the governing equations using a Dirac delta function. A simplified linear dimensionless governing equation has been derived and an analytical solution expressed in terms of a Fourier series has been developed under constant boundary conditions. The linear analysis indicates that pipe friction and a partial blockage both introduce damping on fluid transients. The friction damping and blockage damping are exponential for each of the individual harmonic components. For each individual harmonic component, the blockage-induced damping depends on the blockage magnitude and position and is independent of measurement location and the transient event. A new blockage detection method using the blockage-induced transient damping is developed based on the analytical solution. The magnitude of the blockage-induced damping rate

[1] Project Engineer, Tonkin Consulting, 5 Cooke Terrace, Wayville, SA 5034, Australia. (corresponding author) Email: xiao-jian.wang@tonkin.com.au. Tel: 61.8.8273 3100, Fax: 61.8.8273 3110

[2] Senior Lecturer, Centre for Applied Modelling in Water Engineering, School of Civil & Environmental Engineering, The University of Adelaide, Adelaide, SA 5005, Australia. Email: mlambert@civeng.adelaide.edu.au.

[3] Associate Professor, Centre for Applied Modelling in Water Engineering, School of Civil & Environmental Engineering, The University of Adelaide, Adelaide, SA 5005, Australia. Email: asimpson@civeng.adelaide.edu.au.

indicates the size of the blockage and the ratios of different damping rates can be used to locate the blockage. The proposed blockage detection method has been successfully used in detecting, locating and quantifying a pipe blockage based on laboratory experiments.

Key words: blockage detection, pipe transients, transient damping, pipe friction, Fourier series

Introduction

Blockage development is a common problem in pipeline and pipe network systems for the energy, chemical and water industries. A blockage can be formed by localised chemical or physical deposition, or formed by a negligently partially closed valve. Existence of a pipeline blockage not only reduces the operation efficiency of a pipeline system, but sometimes it can cause severe safety problems if the blockage is not identified in timely manner. Some methods have been proposed previously to detect and locate pipeline blockage. Rogers (1995) developed a ROV (remotely operated vehicle) inspection method by measuring the blockage-induced strain change of the pipe wall. Since this method cannot be applied continuously, the response for a blockage occurrence is slow. Wu (1994) proposed an acoustic method based on the properties of eigenfrequency shifts of acoustic signals measured from a pipeline with a blockage. Due to the quick decay of the acoustic signals, the measurement interval needs to be less than one hundred meters. In petroleum engineering, the development of a blockage has been related to the properties of the fluid in the pipes. Therefore, analyzing the fluid properties can indicate the potential development of the blockage (Hunt 1996). Unfortunately, this method cannot provide the location of the blockage. By analyzing the blockage (or leakage)-induced water head losses, Jiang et al. (1996) developed a blockage and leakage detection algorithm for the water network of a

district heating system. Depending on the measurement locations, only significant leakage and blockages can be detected and located based on the numerical experiments. In the methods developed by Scott and Satterwhite (1998) and Scott and Yi (1999), a blockage was detected and characterized by the mass and momentum (friction loss) balance analysis. A detectable blockage map was developed in Scott and Yi (1999). These methods could not detect the location of a blockage although it was noticed that the transients were affected by the location of the blockage during tests. Adewumi et al. (2000) numerically studied the reflections of gas transients from different shapes of pipeline constrictions. Numerical tests showed that pipeline blockages could be detected from the reflected transients. However, because the magnitudes of the blockage reflections were less than 0.005 psi and were only 0.0005% of the pipeline base pressure, it would be difficult to identify the reflected transients in a real situation. Recently, several leak detection methods using fluid transients in a pipe system have been presented (Liggett and Chen 1994; Brunone 1999; Wang et al. 2002), and have shown considerable advantages of quick response and accuracy when compared to other leak detection methods. Compared to acoustic signals, fluid transients are less influenced by the surrounding environment and can propagate longer distance with less decay, which is advantageous for remote surveillance. As a complement to the leak detection method proposed by Wang et al. (2002), a new blockage detection method using blockage-induced transient damping is developed in this paper. The proposed method is verified using laboratory experiments.

An Analytical Solution

A partial blockage in a pipeline system can be considered as an orifice as shown in Fig. 1. Presence of a partial blockage only influences the momentum equation of unsteady pipe flow

and has no influence on the continuity equation. Governing equations for the unsteady flow in a pipe section including a blockage are expressed as (Wang 2002)

$$\frac{\partial H}{\partial x}+\frac{1}{gA}\frac{\partial Q}{\partial t}+\frac{Q}{gA^2}\frac{\partial Q}{\partial x}+\frac{f\,Q^2}{2DgA^2}-\Delta H_B\delta(x-x_B)=0 \tag{1}$$

$$\frac{\partial H}{\partial t}+\frac{Q}{A}\frac{\partial H}{\partial x}+\frac{a^2}{gA}\frac{\partial Q}{\partial x}=0 \tag{2}$$

where x = distance along the pipe, t = time, H = piezometric head, and Q = the flow rate in the pipeline, D = pipe diameter, g = gravitational acceleration, A = pipe cross-sectional area, a = wave speed in the fluid, x_B = location of the blockage, ΔH_B = head loss across the blockage, f = pipe friction factor, and δ = Dirac delta function defined by (4) and (5).

Eq. (2) assumes that pipe friction during a transient event is described by a constant steady-state Darcy-Weisbach friction factor. The main objective in considering the solution to this set of governing equations is to understand the influence of a blockage on a transient event. However, it is known that pipe friction during a transient event is significantly larger than that predicted by the constant Darcy-Weibach friction factor due to unsteady friction. The effects of unsteady friction are introduced into the solution once the governing equations have been developed based on the same approach as for the leaks by Wang et al. (2002). Details of this approach are given later in the paper.

The head across the blockage may be expressed as

$$\Delta H_B=\frac{K_B Q^2}{2gA^2} \tag{3}$$

where K_B is the head loss coefficient of the blockage and is used as the indicator of the blockage size. If the flow rate is known, the blocked-pipe cross-sectional area or diameter of the blockage can be estimated from K_B (Miller, 1978).

In (1), the Dirac delta function is defined as

$$\delta(x - x_B) = \begin{cases} \infty & \text{if} \quad x = x_B \\ \\ 0 & \text{otherwise} \end{cases} \tag{4}$$

so that $$\lim_{\varepsilon \to 0} \int_{x_B - \varepsilon}^{x_B + \varepsilon} \delta(x - x_B)\, dx = 1 \tag{5}$$

in which ε = a small distance on the either side of the blockage. Although a pipeline blockage typically has a finite length (in the order of several meters), approximation using a delta function is reasonable for a long pipeline of several kilometers. If the length of a blockage is not negligible compared to the length of the pipeline, then the delta-function approach is not valid.

The following quantities are used to non-dimensionalize (1), (2) and (3):

$$h^*(x^*, t^*) = \frac{H(x,t) - H_0(x)}{H_S}, \quad q^*(x^*, t^*) = \frac{Q(x,t) - Q_0}{Q_0},$$

$$t^* = \frac{t}{L/a}, \quad x^* = \frac{x}{L}, \text{ and} \tag{6}$$

$$\delta(x^* - x_B^*) = \delta(x - x_B) L$$

in which h^* = a non-dimensional head deviation, H_0 = steady-state head, q^* = a non-dimensional flow deviation, Q_0 = steady flow, L = the pipe length, and $H_s = \frac{aV_0}{g}$ is the Joukowsky pressure head rise. Substituting (3) and (6) into (1) and (2), and neglecting the convection terms as in the standard development of the method of characteristics equations gives the simplified dimensionless equations as

$$\frac{\partial h^*}{\partial t^*} + \frac{\partial q^*}{\partial x^*} = 0 \tag{7}$$

$$\frac{\partial h^*}{\partial x^*} + \frac{\partial q^*}{\partial t^*} + [R + G\delta(x^* - x_B^*)](2q^* + q^{*2}) = 0 \tag{8}$$

in which

$$R = \frac{fLQ_0}{2DaA}, \text{ and } G = \frac{K_B Q_0}{2aA} \tag{9}$$

where R = friction damping factor, and G = blockage resistance parameter.

Although a governing equation in h^* is preferred (the measurement of transient pressures is more accurate than measurement of the transient flow rates), due to the presence of the delta function in (8) and the difficulty in finding the x-derivative of the delta function, the variable q^* cannot be eliminated. Applying the operation $\frac{\partial[\text{Eq. (7)}]}{\partial x^*} - \frac{\partial[\text{Eq. (8)}]}{\partial t^*}$ gives the governing equation in q^* as

$$\frac{\partial^2 q^*}{\partial x^{*2}} = \frac{\partial^2 q^*}{\partial t^{*2}} + [2R + 2G\delta(x^* - x_B^*)](1 + q^*)\frac{\partial q^*}{\partial t^*} \tag{10}$$

The last term on the right hand side of (10) is non-linear. For a small transient where $q^* << 1.0$ (the influence of this assumption is investigated in the later section), (10) may be simplified to

$$\frac{\partial^2 q^*}{\partial x^{*2}} = \frac{\partial^2 q^*}{\partial t^{*2}} + [2R + 2G\delta(x^* - x_B^*)]\frac{\partial q^*}{\partial t^*} \tag{11}$$

For a pipeline connecting two reservoirs with constant water elevations

$$h^*(0\ ,\ t^*) = 0 \text{ and } h^*(1\ ,\ t^*) = 0 \tag{12}$$

Substituting (12) into the continuity equation (7) gives flow boundary conditions

$$\frac{\partial q^*(0,t^*)}{\partial x^*} = 0 \quad \text{and} \quad \frac{\partial q^*(1,t^*)}{\partial x^*} = 0 \tag{13}$$

If a known transient has been initiated in the pipeline, the initial flow conditions are given as

$$q^*(x^*,0) = f_q(x^*) \text{ and } \frac{\partial q^*(x^*,0)}{\partial t^*} = g_q(x^*) \tag{14}$$

Although these initial conditions would likely be impossible to define for a real pipeline, it does not matter because they are not needed when the problem is transformed to be in terms of head by integrating the continuity equation (see Eq. (20)).

By applying a Fourier expansion (Wang 2002), the solution of (11) subject to the boundary conditions in (13) is

$$q^*(x^*,t^*) = \sum_{n=1}^{\infty} \left\{ e^{-(R+R_{nB})t^*} \left[(A'_n \cos(n\pi t^*) + B'_n \sin(n\pi t^*) \right] \cos(n\pi x^*) \right\} \tag{15}$$

in which

$$R_{nB} = 2G\cos^2(n\pi x_B{}^*) \tag{16}$$

where R_{nB} is the blockage damping factor for Fourier component n , and $x_B{}^*$ = dimensionless blockage location along the pipeline. The values of the Fourier coefficients in (15) are calculated using the initial conditions as

$$A'_n = 2\int_0^1 f_q(x^*)\cos(n\pi x^*)dx^* \quad (n = 1, 2, 3,.....) \tag{17}$$

$$B'_n = \frac{1}{n\pi}[\int_0^1 2g_q(x^*)\cos(n\pi x^*)dx^* + A_n(R + R_{nB})] \quad (n = 1, 2, 3,.....) \tag{18}$$

The solution for transient head is obtained by integrating the continuity equation (7) with respect to t^* as

$$h^*(x^*,t^*) = \int -\frac{\partial q^*(x^*,t^*)}{\partial x^*} dt^* \tag{19}$$

Substituting (15) into (19) gives

$$h^*(x^*,t^*) = \sum_{n=1}^{\infty} \left\{ e^{-(R+R_{nB})t^*} \left[A_n \cos(n\pi t^*) + B_n \sin(n\pi t^*) \right] \sin(n\pi x^*) \right\} \tag{20}$$

where Fourier coefficients A_n and B_n can be determined from initial conditions on pipeline pressure, which can be expressed as

$$h^*(x^*,\ 0) = f_h(x^*) \text{ and } \frac{\partial h^*(x^*,0)}{\partial t^*} = g_h(x^*) \tag{21}$$

and $$A_n = 2\int_0^1 f_h(x^*) \sin(n\pi x^*) dx^* \quad (n = 1, 2, 3,...) \tag{22}$$

$$B_n = \frac{2}{n\pi} \int_0^1 g_h(x^*) \sin(n\pi x^*) dx^* + \frac{(R + R_{nB}) A_n}{n\pi} \quad (n = 1, 2, 3,...) \tag{23}$$

Unsteady friction

In the derivation of (1), the friction loss was assumed to be represented by a steady-state friction factor. For the rapidly varying flow, experiments have shown that the damping of transients is greater than that predicted by the steady-state friction factor. This difference can be addressed by using an unsteady friction model, such as Zielke (1968), Brunone et al. (1995), Vardy and Brown (1996) or Bergant et al. (2001). Applying an unsteady friction model, the total friction is expressed as

$$f = f_s + f_u \tag{24}$$

where f_s =steady-state friction factor, and f_u = unsteady friction factor. To account the unsteady friction effects, the friction-damping factor in (20) is replaced by

$$R = R_s + R_u \tag{25}$$

in which R_s = steady friction damping factor and R_u = unsteady friction damping factor. Therefore, the solution for the transient in a pipeline with a partial blockage is modified as

$$h^*(x^*,t^*) = \sum_{n=1}^{\infty} \left\{ e^{-(R_s+R_u+R_{nB})t^*} \left[A_n \cos(n\pi t^*) + B_n \sin(n\pi t^*) \right] \sin(n\pi x^*) \right\} \tag{26}$$

The values of friction damping factors (R_s and R_u) can be determined from a transient test in a blockage-free pipeline. Alternatively the steady friction damping factor can be calculated from the steady-state flow condition ($R_s = \frac{f_s L Q_0}{2DA}$), and the unsteady friction damping may be obtained from the unsteady friction modelling (Bergant et al. 1999). The steady friction damping factor is a function of pipeline system parameters including pipe length, pipe diameter, steady-state flow rate and pipe friction factor. The steady friction damping factor is independent of the transient event and is the same for all the different Fourier components. To the contrary, the unsteady friction damping factor is component-dependent.

Application for blockage detection

Eq. (26) shows that a measured transient (under the condition of q^*<<1) in a pipeline that includes a blockage is the summation of a series of harmonic components that are each exponentially damped with the damping rate of $R_s + R_u + R_{nB}$ (n = 1, 2, 3,…). The blockage damping factor (R_{nB}) is a function of blockage magnitude and location and is independent of the transients and pipe flow conditions. For a measured pipe transient, the damping rates ($R_s + R_u + R_{nB}$) of individual components can be obtained by decomposing the transient into a

Fourier series (Wang et al. 2002). The blockage damping factor R_{nB} can be found by subtracting friction damping ($R_s + R_u$) from $R_s + R_u + R_{nB}$.

Presence of a pipeline blockage may be indicated by the increased damping rates compared to the friction damping rates ($R = R_s + R_u$) obtained from a blockage-free pipeline or an unsteady model. The location of the blockage can be determined by the ratio of two damping rates. For each of the Fourier components, the blockage-induced damping is a function of blockage magnitude and location. However, the ratio of any two blockage-induced damping parameters defined in (16) is a function of blockage location only, which can be expressed as

$$\frac{R_{n_2B}}{R_{n_1B}} = \frac{\cos^2(n_2\pi x_B^*)}{\cos^2(n_1\pi x_B^*)} \tag{27}$$

Fig. 2 is a plot of the theoretical relationship between the damping ratios of harmonic components $n_2 = 2$, $n_1 = 1$ and harmonic components $n_2 = 3$, $n_1 = 1$ with the corresponding blockage locations in a pipeline. Due to the symmetric nature of the cosine squared function, the relationship between the damping ratio of two harmonic components and the blockage location is not unique. Two or up to four blockage locations correspond to one value of the damping ratio R_{2B}/R_{1B} except for $x_B^* = 0.5$, which is a unique point because the blockage damping $R_{1B} = 0$ at $x_B^* = 0.5$. For the damping ratio of higher harmonic components, one damping ratio corresponds to more possible blockage locations; therefore, only harmonic components of $n < 4$ are used for blockage detection analysis in this study.

Once the position of the blockage has been determined, the blockage magnitude can be easily calculated based on (9) and (16). It is

$$G = \frac{R_{nB}}{2\cos^2(n\pi x_B^*)} = \frac{K_B Q_0}{2aA} \qquad (n = 1, 2, 3,\ldots) \qquad (28)$$

where n is any one of the components. Theoretically, the blockage magnitude calculated using different components should be the same. Different measurement positions and different forms of transients can be used for added confirmation and to increase accuracy if necessary.

Sensitivity analysis

The application of the proposed blockage detection method depends on the accuracy of the values of blockage damping on individual Fourier components. In the derivation of (11), the q^* value was assumed small ($q^* << 1.0$). The influence of the transient magnitude on the blockage-induced damping and thus on the blockage detection including location and magnitude is investigated in this section.

Assuming a constant q^* gives the approximate solution as

$$h^*(x^*, t^*) = \sum_{n=1}^{\infty} \left\{ e^{-(R'+R'_{nB})t^*} \left[A_n \cos(n\pi t^*) + B_n \sin(n\pi t^*) \right] \sin(n\pi x^*) \right\} \qquad (29)$$

where $R' = (1+q^*)(R_s+R_u)$, and $R'_{nB} = (1+q^*)R_{nB}$. The apparent blockage damping for the n^{th} component n is $(R_{nB})_{apparent} = (1+q^*)R_{nB}$. As the blockage location is related to the ratio of two blockage damping factors, the influence of transient magnitude on the blockage location cancels out (see (27)). Therefore, the transient magnitude q^* has little influence on the detection of the blockage location.

The error in blockage magnitude induced by the orifice linearization is defined as

$$\varepsilon_s = \frac{G_{apparent} - G_{real}}{G_{real}} = q^* \tag{30}$$

Eq. (30) indicates that the error in the sizing of blockage is proportional to the transient magnitude.

Since blockage-induced damping is obtained from total damping of a transient component by subtracting the friction damping, the error in calculating friction damping will be transferred to the estimate of blockage-induced damping and, as a result, the outcome of blockage detection may be affected. If there is an error ΔR in measuring (or calculating) the friction damping factor ($R_{error} = \Delta R + R_s + R_u$), the contaminated blockage-induced damping on n^{th} harmonic component is R_{nB}-ΔR. Assuming that error of friction damping is the same for different harmonic components, the ratio of two blockage-induced damping coefficients for any two components is

$$\frac{R_{n_2B} - \Delta R}{R_{n_1B} - \Delta R} = \frac{\cos^2[n_2\pi(x_L^* + \varepsilon_L)]}{\cos^2[n_1\pi(x_L^* + \varepsilon_L)]} \tag{31}$$

where ε_L = dimensionless distance away from a real leak location. Substituting $\frac{R_{n_2B}}{R_{n_1B}} = \frac{\cos^2(n_2\pi x_L^*)}{\cos^2(n_1\pi x_L^*)}$ into (31) and rearranging gives

$$\frac{\frac{\cos^2(n_2\pi x_L^*)}{\cos^2(n_1\pi x_L^*)} - S_f}{1 - S_f} = \frac{\cos^2[n_2\pi(x_B^* + \varepsilon_L)]}{\cos^2[n_1\pi(x_B^* + \varepsilon_L)]} \tag{32}$$

where $S_f = \frac{R\Delta f}{2R_{n_1 B} f}$ = sensitivity parameter of the friction damping factor. The blockage location error, ε_L, is a function of parameter S_f and real blockage location, x_B^*. Similarly, the error in the magnitude of a blockage caused by the friction factor uncertainties is expressed as

$$\varepsilon_s = \frac{(G_B)_{real} - (G_B)_{apprarent}}{(G_B)_{real}} = 1 - \frac{(1 - S_f)\cos^2(n\pi x_B^*)}{\cos^2[n\pi(x_B^* + \varepsilon_L)]} \tag{33}$$

Variations of blockage location error (ε_L) and magnitude error (ε_S) caused by the pipe friction uncertainties are plotted in Fig. 3 and Fig. 4 respectively. Errors in both the blockage location and the magnitude increase with an increase of the pipe friction uncertainty parameter S_f. In addition, pipe friction uncertainty has a more significant influence on blockage magnitude than on blockage location. For a parameter of S_f = 0.1, the blockage location may be influenced by 4% while influence on blockage magnitude may be up to 30%. Because the error of both the location and the magnitude is proportional to parameter S_f, higher values of blockage damping factor (R_{nB}) will improve the blockage detection based on the proposed method. Therefore, a higher steady pipe flow rate (Q_0) which will result in a higher blockage damping factor will generate better performance based on the definition of R_{nB} in (9) and (16). This is different to the leak detection, in which the detectability of a leak is affected by the pressure in the pipeline (Wang et al. 2002). In order to produce the best blockage detection performance, blockage detection tests using the proposed method should be conducted at a reasonable flow rate that creates a measurable head loss across the blockage. If the steady-state head loss across the blockage is very small, the blockage-induced transient damping will be small. The measurement of blockage damping will be contaminated by background noises and the blockage location and quantification using the proposed method will not be accurate.

In addition, as rapid (not necessarily large) transients contain more harmonics than the slow transients, blockage detection using rapid transients can provide more information of damping factors of different harmonics. As a result, blockage detection using a rapid transient can improve the accuracy of both location and sizing based on the proposed method.

Laboratory experimental verification

Experimental tests were conducted in a single pipeline in the Robin Hydraulics Laboratory at the University of Adelaide to verify the practical feasibility of the proposed blockage detection method. The experimental setup is shown in Fig. 5. A blockage is simulated by a partially closed valve (Valve 1) located near the Tank 1.

Two tests were conducted. Test I is a no–blockage case (Valve 1 is fully open) and in Test II, the Valve 1 is partially closed. The flow conditions are as follows:

Length of the pipeline	L = 37.2 m,
Pipe diameter	D = 0.022 m,
Thickness of the pipe wall	e = 1.6 mm,
Wave speed	a = 1,320 m/s,

In both Test I and Test II, the heads at two tanks are set as H_1 = 27.53m, and H_2 = 26.60m. In Test I, the Valve 1 is fully open, and the steady flow velocity in the pipeline was V_0 = 0.80 m/s. Given the Reynolds number of Re = 15,400, the Darcy-Weisbach friction factor is calculated as f = 0.017 (smooth pipe) and the steady friction damping factor is calculated as R_s = 0.0087. In Test II, the Valve 1 is partially closed, the steady flow in the pipeline is reduced to V_0 = 0.36 m/s (Re = 7,920), and the steady friction damping factor is calculated as R_s =

0.0036. Based on the total head loss and the steady flow in the pipeline, the head loss coefficient of the partially closed Valve 1 is calculated as $K_B = 114.9$.

In Test I, the valves at locations A and E and the side-discharge valve at D are fully opened and a steady state condition is achieved. The side-discharge solenoid valve at D is then closed quickly. In Test II, the valve 1 at A is partially closed, and the valve at location E is fully open. The side-discharge valve at D is opened until steady state conditions are obtained. The side-discharge valve at D is then sharply closed. The flow rate at the side-discharge is 3.8×10^{-5} m^3/s for both tests. The flow disturbance ($q^* = q/Q_0$) is approximately 6% and 13% for Test I and Test II respectively. During the tests, pressures are measured by five pressure transducers at points A, B, C, D, and E. Measured pressures in the middle of the pipeline ($x^* = 0.50$) from both Test I and Test II are plotted in Fig. 6(a) and are used for blockage detection analysis. The blockage-induced damping of Test II is obvious compared to the transient in Test I that has no blockage.

By applying a discrete Fourier transform algorithm to decompose the measured data (see Wang et al. 2002), the amplitude for the separate components are presented in Fig. 6(b). Each component was fitted to an exponential function, and the damping coefficient of each component was calculated. The damping coefficients of the first three components (n = 1, 2, 3) for both Test I and Test II are presented in Fig. 6(c). For the no-blockage case (Test I), steady and unsteady friction damping factors of the first three harmonic components are $R_s + R_{1u} = 0.0213$, $R_s + R_{2u} = 0.0476$, $R_s + R_{3u} = 0.0735$, all being larger than the steady friction damping factor $R_s = 0.0087$, calculated using steady state friction. The differences between the measured and the calculated damping values are due to unsteady friction. Unsteady

friction damping factors for the first three components are R_{1u} = 0.0126, R_{2u} = 0.0389, R_{3u} = 0.0648, which account for approximately 59%, 82% and 88% of the total damping.

In Test I and Test II, since the transients were initiated by closing the side-discharge valve in the same amount of time and the flows in both tests are turbulent flows, the unsteady friction damping effects are approximately the same. Therefore, in Test II the friction damping factors for the first three components are $R_s + R_{1u}$ = 0.0161, $R_s + R_{2u}$ = 0.0424 and $R_s + R_{3u}$ = 0.0683. By subtracting the steady and unsteady friction damping from the total damping, blockage-induced damping coefficients for the first three components (n = 1, 2, 3) are R_{1B} = 0.0472, R_{2B} = 0.0466, R_{3B} = 0.0469. The ratios of damping coefficients R_{2B} and R_{1B}, and R_{3B} and R_{1B} are $\frac{R_{2B}}{R_{1B}} = 0.994$, and $\frac{R_{3B}}{R_{1B}} = 0.994$. Corresponding blockage locations for these damping ratios are x_B^* = 0.0 (or x_B^* = 1.0) by applying these two ratios in Fig. 2. This is same as the real blockage location x_B^* = 0.0. Using R_{1B} = 0.0472, R_{2B} = 0.0466 and leak location x_B^* = 0.0, the head loss coefficient for the blockage is calculated from (28), as K_B = 188.8. The value of the head loss coefficient calculated from the transient experiment is about 40% larger than that based on steady-state test of K_B = 114.9.

Conclusions

The behavior of a blockage on pipeline transients has been studied in this paper. The analytical solution indicates that transients in pipelines are damped by both friction and blockages. Blockage-induced damping is exactly exponential for each of the individual harmonic components. Compared to leak-induced damping, which is related to pressure in the pipeline and is independent of flow rate in the pipeline, blockage damping is proportional

to flow rate, and does not have a direct relationship with the pressure in the pipeline. Therefore, in order to produce the best blockage detection performance, blockage detection tests should be conducted at a reasonable flow rate that creates a measurable head loss across the blockage. In addition, blockage-induced transient damping and leak-induced transient damping have different modes (Wang et al. 2002). The relationship between blockage location and blockage damping is a cosine-squared function while leak location and leak damping is a sine-squared function. As a result, a blockage close to the reservoir in a reservoir-pipeline-reservoir system is more easily detected compared to the other locations while a leak in the middle of the pipeline is more easily detected (Wang et al. 2002). Because rapid transients have more harmonics, blockage detection using a rapid transient will improve blockage detection performance.

Sensitivity analyses have shown that the accuracy of blockage detection using the method presented in this paper is influenced by transient magnitude, and the accuracy of the pipe friction damping factor. These factors have a more significant influence on the blockage magnitude than on the blockage location. Theoretically, a smaller transient magnitude will produce better blockage detection performance; however, this will depend on the level of noise of the measured signals. The proposed blockage detection technique is simple to use and apply; however, this method may not be applicable in complex systems such as pipe networks. In addition, due to the difficulty to model the unsteady pipe friction, transient tests for a blockage-free condition are needed to obtain the unsteady friction damping factor. Therefore, the proposed method would be suitable in the field for a new pipeline in which a blockage grows but not suitable in an older pipeline where an existing blockage has developed.

Acknowledgements

The research presented in this paper has been supported by the Australian Research Council Discover Grant funded by the Australian Government and the University of Adelaide through an overseas student scholarship to the first author.

References

Adewumi, M. A., Eltohami, E. S., and Ahmed, W. H. (2000). "Pressure transients across constrictions." *Journal of Energy Resources Technology*, ASME, 122, 34-41.

Bergant, A., Simpson, A. R., and Vitkovsky, J. (2001). "Developments in unsteady pipe flow friction modelling." *Journal of Hydraulic Research*, IAHR, 39(3), 249-257.

Brunone, B. (1999). "Transient test-based technique for leak detection in outfall pipes." *Journal of Water Resources Planning and Management,* ASCE, 125(5), 302-306.

Brunone, B., Golia, U. M., and Greco, M. (1995). "Effects of two-dimensionality on pipe transients modeling." *Journal of Hydraulic Engineering,* ASCE, 121(12), 906-912.

Hunt, A. (1996). "Fluid properties determine flow line blockage potential." *Oil & Gas Journal*, 94(29, July 15), 62-66.

Jiang, Y., Chen, H., and Li, J. (1996). "Leakage and Blockage detection in water network of district heating system." ASHRAE *Transactions*, 102(1), 291-296.

Liggett, J. A., and Chen, L.-C. (1994). "Inverse transient analysis in pipe network." *Journal of Hydraulic Engineering,* ASCE, 120(8), 934-955.

Miller, D. S. (1978). *Internal Flow Systems*, BHRA Fluid Engineering.

Rogers, L. M. (1995). "Pipeline blockage location by strain measurement using an ROV." *Proceedings of the 1995 Offshore Technology Conference*, Houston, TX, USA, 521-528.

Scott, S. L., and Satterwhite, L. A. (1998). "Evaluation of the back pressure technique for blockage detection in gas flowlines." *Journal of Energy Resources Technology,* ASME, 120, 27-31.

Scott, S. L., and Yi, J. (1999). "Flow testing methods to detect and characterize partial blockages in looped subsea flowlines." *Journal of Energy Resources Technology,* ASME, 121, 154-160.

Vardy, A. E., and Brown, J. (1996). "On turbulent, unsteady, smooth-pipe friction." *Conference on Pressure Surges and Fluid Transients, Durham,* UK, 289-311.

Wang, X.-J. (2002). *Leak and Blockage Detection in Pipelines and Pipe Network Systems Using Fluid Transients*, Ph.D. Thesis, School of Civil & Environmental Engineering, The University of Adelaide, Adelaide, Australia.

Wang, X.-J., Lambert, M. F., Simpson, A., R., Liggett, J. A., and Vítkovský, J. P. (2002). "Leak detection in pipelines using the damping of fluid transients." *Journal of Hydraulic Engineering,* ASCE, 128(7), 697-711.

Wu, Q. (1994). "Reconstruction of blockage in a duct from single spectrum." *Applied Acoustics*, 41(3), 229-236.

Wylie, E. B., and Streeter, S. L. (1993). *Fluid Transients in Systems*, Prentice-Hall Inc., Englewood Cliffs, New Jersey, USA.

Zielke, W. (1968). "Frequency-dependent friction in transient pipe flow." *Journal of Basic Engineering*, ASME, 90, 109-115.

Notation

A	=	inner pipe cross-sectional area (m^2);
A_n, B_n	=	Fourier coefficients;
A_n', B_n'	=	Fourier coefficients;
a	=	wave speed (m/s);
D	=	pipe diameter (m);
e	=	thickness of pipe wall (mm);
f	=	friction factor;
f_s	=	Darcy-Weisbach steady friction factor;
f_u	=	unsteady friction factor;
G	=	blockage resistance parameter;
$G_{apparent}$	=	apparent blockage resistance parameter;
g	=	gravitational acceleration (m/s^2);
H	=	piezometric head (m);
H_0	=	steady state piezometric head (m);
H_1, H_2	=	heads at reservoirs (m);
H_s	=	Jouskowsky pressure head rise (m);
H^*	=	dimensionless head $=H/H_1$;
h^*	=	dimensionless head disturbance;
K_B	=	blockage head loss coefficient;
L	=	length of pipeline (m);
n	=	component number in a Fourier series;
Q	=	flow rate (m^3/s);

Q_0 = steady state flow rate (m^3/s);

Q^* = dimensionless flow rate $=Q/Q_0$;

q^* = dimensionless flow rate disturbance;

$R,\ R'$ = pipeline friction damping factor; linear regression parameter;

R_s = steady friction damping factor;

R_u = unsteady friction damping factor;

Re = Reynolds number;

R_{nB}, R'_{nB} = blockage damping factor for n^{th} harmonic (n = 1,2,3,…);

S_f = sensitivity parameter for friction factor;

T = natural period of pipeline = L/a (s);

t = time (s);

t^* = dimensionless time = $t/(L/a)$;

V_0 = steady flow velocity in pipe (m/s);

x = distance along pipeline;

x^* = dimensionless distance = x/L;

x_B = position of blockage;

x_B^* = dimensionless blockage position = x_B/L;

ΔH_B = blockage-induced head loss;

ΔR = friction damping error;

δ = Dirac delta function;

ε = roughness height for pipe wall; a small distance from the leak (m);

ε_L = dimensionless blockage location error;

ε_S = dimensionless blockage size error;

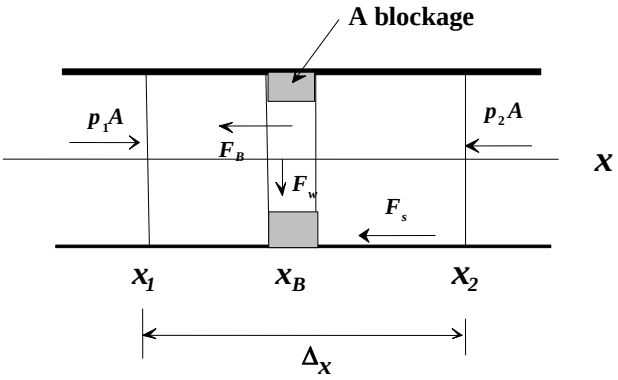

Fig. 1 Free-body diagram for a pipe section with a blockage

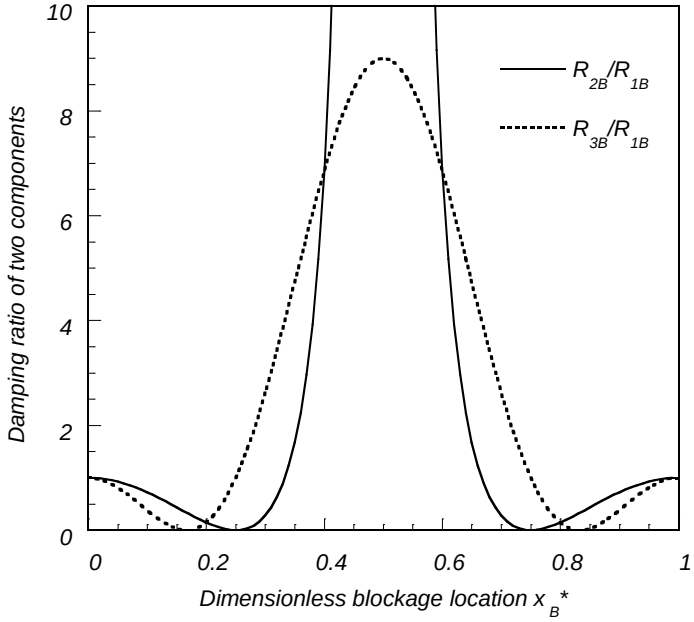

Fig. 2 Ratio of blockage damping coefficients of two Fourier components

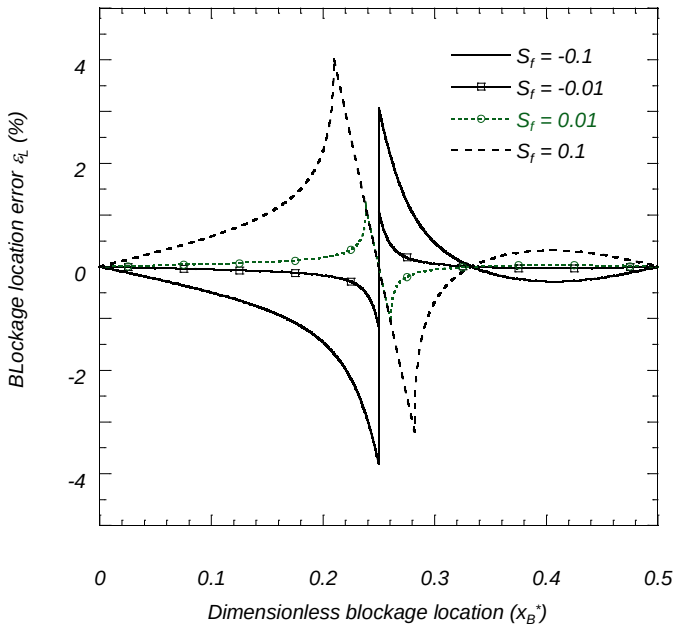

Fig. 3 Error of blockage location caused by the pipe friction uncertainty

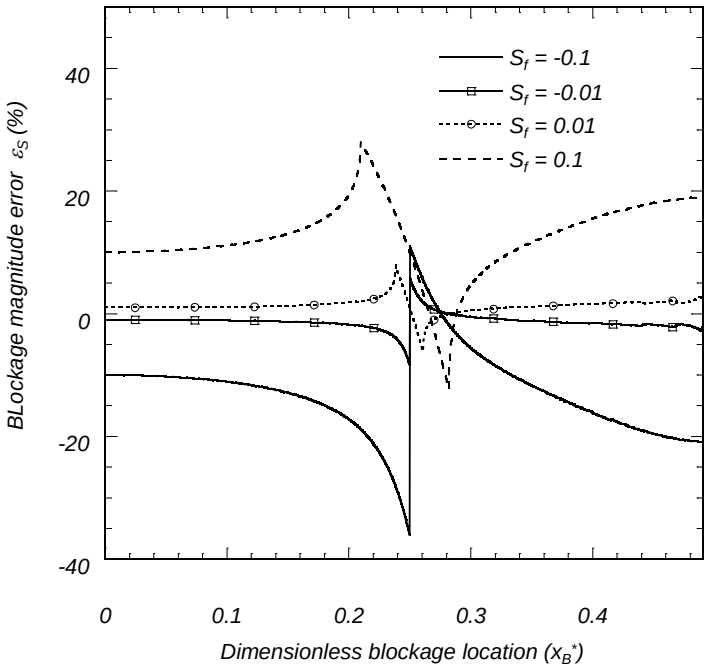

Fig. 4 Error of blockage magnitude caused by the pipe friction uncertainty

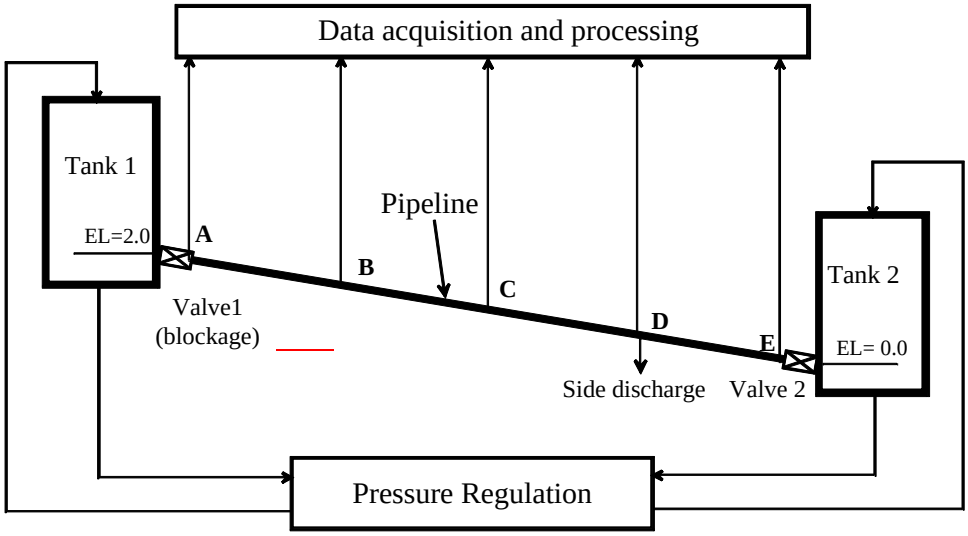

Fig. 5 Laboratory setup for blockage detection

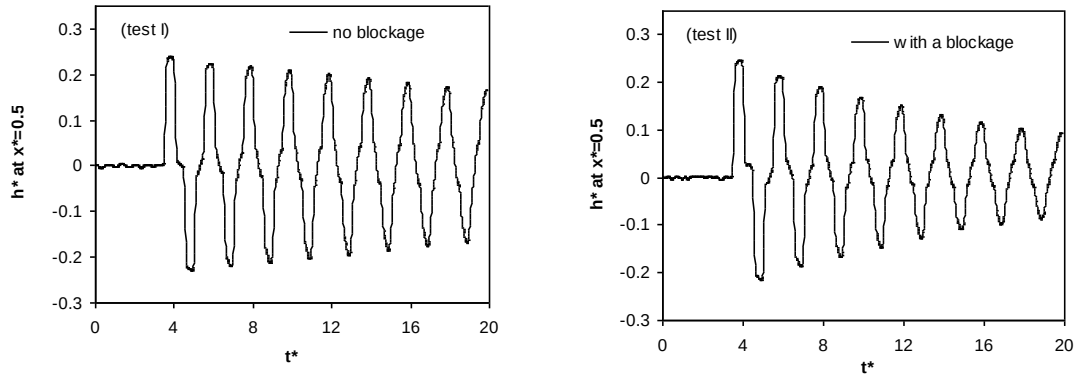

(a) Measured transients

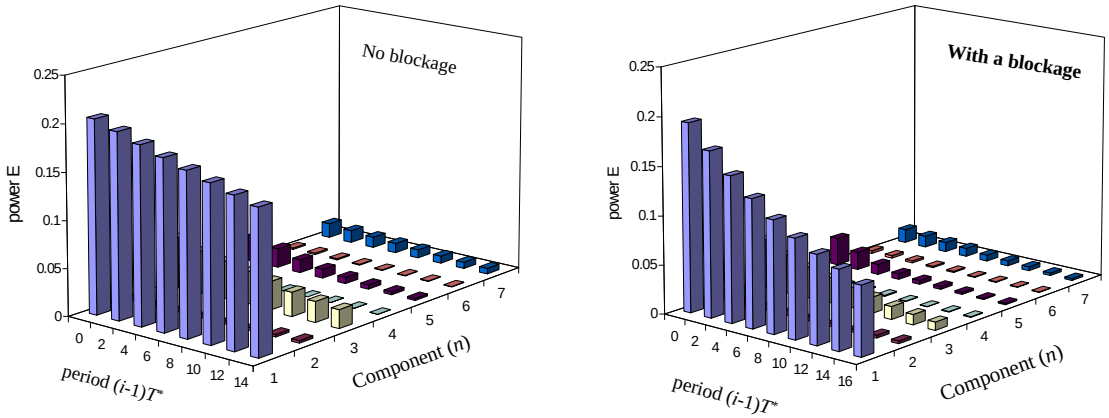

(b) Frequency analysis

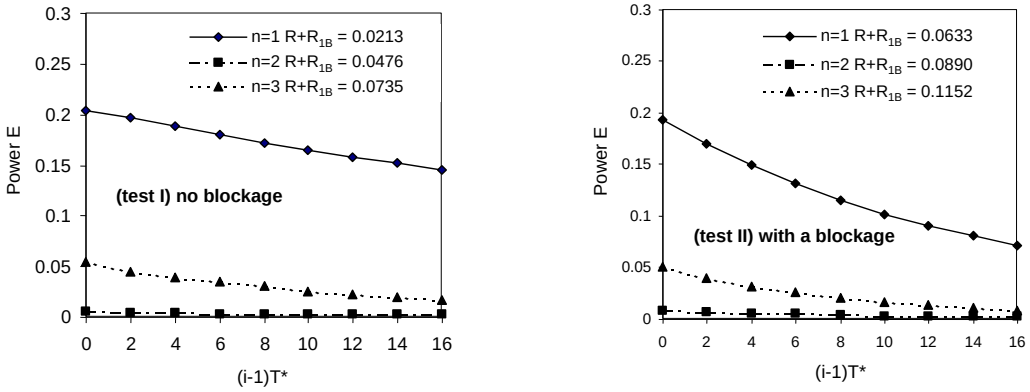

(c) Damping analysis ($R = R_s + R_u$)

Fig. 6 Laboratory experimental verification of blockage detection

Fig. 1 Free-body diagram for a pipe section with a blockage

Fig. 2 Ratio of blockage damping coefficients of two Fourier components

Fig. 3 Error of blockage location caused by the pipe friction uncertainty

Fig. 4 Error of blockage magnitude caused by the pipe friction uncertainty

Fig. 5 Laboratory setup for blockage detection

Fig. 6 Laboratory experimental verification of blockage detection

(a) Measured transients; (b) Frequency analysis; (c) Damping analysis ($R = R_s + R_u$)